








RESEARCH ARTICLE

Nanostructured scaffolds containing graphene oxide for nanomedicine applications

Thiers M. Uehara¹  | Fernanda L. Migliorini¹  | Murilo H. M. Facure^{1,2}  |
 Nicolau B. Palma Filho³  | Paulo B. Miranda³  | Valtencir Zucolotto³  |
 Daniel S. Correa^{1,2} 

¹Nanotechnology National Laboratory for Agriculture (LNNA), Embrapa Instrumentação, São Paulo, Brazil

²PPGQ, Department of Chemistry, Center for Exact Sciences and Technology, Federal University of São Carlos (UFSCar), São Paulo, Brazil

³Physics Institute of São Carlos, University of São Paulo, São Paulo, Brazil

Correspondence

Thiers M. Uehara and Daniel S. Correa, Nanotechnology National Laboratory for Agriculture (LNNA), Embrapa Instrumentação, 13560-970, São Carlos, São Paulo, Brazil. Email: tmuehara@gmail.com and daniel.correa@embrapa.br

Funding information

AgroNano Research; Conselho Nacional de Desenvolvimento Científico e Tecnológico, Grant/Award Numbers: 155449/2018-4, 155449/2016-2; Coordenação de Aperfeiçoamento de Pessoal de Nível Superior, Grant/Award Number: Funding Code 001; Fundação de Amparo à Pesquisa do Estado de São Paulo, Grant/Award Numbers: 2017/10582-8, 2018/02819-0, 2017/21791-7, 2017/12174-4; MCTI-SisNano, Grant/Award Number: CNPq/402.287/2013-4

[Corrections made on 23 November 2021, after first online publication: The ORCID of Murilo H. M. Facure, Nicolau B. Palma Filho, Paulo B. Miranda, and Valtencir Zucolotto have been added in this version.]

Abstract

The use of graphene oxide (GO) has become widespread due to its advantageous properties for applications in medical devices, including cell scaffolds and sensors. Investigations on the spectroscopic and electrochemical features of nanostructured cell scaffolds may be of interest to design novel scaffold architectures aimed at understanding their interactions with healthy and cancer cells. In this study, we investigated the interactions between liver cancer cells and two GO-containing scaffold platforms, namely: cells membrane models containing GO in the form of Langmuir–Blodgett films, and GO-modified biodegradable polycaprolactone nanofibers. Sum-frequency generation spectroscopy revealed the presence and formation of an expanded phospholipid monolayer underneath GO, while scanning electron microscopy images revealed the morphology of the cells on the different surfaces. Electrochemical impedance spectroscopy was employed to evaluate the charge transfer resistance in different nanostructured scaffolds containing liver cancer cells. The nanosystems developed here can be applied to study the interactions between cells on polymer nanofibers and Langmuir–Blodgett films modified with GO for regenerative medicine.

KEYWORDS

cell membrane model, electrochemical impedance spectroscopy, electrospinning, graphene oxide, Langmuir–Blodgett

1 | INTRODUCTION

Nanotechnology has led to the development of novel nanomaterials with unique physicochemical properties.^{1–5} Graphene oxide (GO) and its derivatives, in particular, are important nanomaterials with enhanced mechanical,⁶ optical,⁷ thermal,⁸ and electrical⁹ properties. Currently, different applications for GO have been proposed, including in

electronic devices and sensors for health monitoring.^{10–13} Nanofibers produced via the electrospinning technique represent an attractive nanoarchitecture model, allowing the development of nanocomposites with different sizes, shapes, morphologies, and functionalities,^{14–16} resulting in 3D mats.^{17,18} This technique has been applied in advanced medicine in mimicked artificial implants, organs, and models for regenerative medicine.^{19,20}

Several strategies have been employed to investigate cancer cells using nanomaterials. For instance, Zheng et al.²¹ developed a label-free method to detect folate receptor-positive tumor cells (Hela and HL 60) using a polydopamine-coated carbon nanotubes-folate nanoprobes, which could bind to cell-surface folate receptors. An electrochemical impedance spectra (EIS) was employed to monitor changes in electron transfer resistance, which sensitive impedance sensor could detect as low as 500 cells.

The understanding of the interactions between cancer cells and different ligands (nanomaterials, biomolecules, and polymers) used as cell scaffolds is crucial for medicine and toxicological studies.^{22,23} Studies on the influence of nanostructured GO-modified scaffolds on liver cancer cells cultures have not been reported so far. In this article we investigated the behavior of liver cancer cells on (HepG2 cells) cultured on two mimicked scaffolds systems, namely: (i) Langmuir-Blodgett film containing cells membrane models and GO, and (ii) GO-modified biodegradable polycaprolactone nanofibers (PCL nanofibers). We evaluated the GO influence on the scaffolds surface containing different nanostructures (PCL nanofibers, GO, GO/PCL nanofibers, 1,2-distearoyl-sn-glycero-3-phosphocholine (DSPC) monolayer, and GO/DSPC monolayer), characterizing their physical/chemistry properties surface, and the charge transfer resistance (R_{ct}) of cancer liver cells at different cells density (5×10^2 , 5×10^3 , and 5×10^4 cells cm^{-2}).

2 | EXPERIMENTAL

2.1 | GO synthesis

Graphite flakes and potassium permanganate (KMnO_4) were obtained from Dinâmica, Brazil. Hydrochloric acid (HCl), sulfuric acid (H_2SO_4), and hydrogen peroxide (H_2O_2) were purchased from Synth Chemical, Brazil. GO synthesis was carried out following an eco-friendly modified Hummers method.²⁴⁻²⁶ Briefly, graphite powder (3 g) was dissolved in H_2SO_4 (70 ml) in an ice bath. To maintain the temperature of the synthesis below 20°C , KMnO_4 (9 g) was slowly added to the mixture. After complete dissolution, the temperature was raised and kept at 40°C for 30 min. Then, 150 ml of double-distilled water was added to the mixture. The solution was maintained at 95°C in an oil-bath for 15 min with continuous stirring. Next, 500 ml of Milli-Q water was added followed by the addition of H_2O_2 (15 ml, 30%),

TABLE 1 Illustration of the composition of nanostructured scaffolds

Scaffolds composition	Nomenclature used
Graphene oxide	GO
1,2-distearoyl-sn-glycero-3 phosphocholine	DSPC monolayer
Polycaprolactone nanofibers	PCL nanofibers
Liver tumor cells	HepG2 cells

causing a color change of the mixture from brown to yellow. The mixture was then filtered and washed with an aqueous solution of HCl (5%) and double-distilled water to remove unreacted reagents and the excessive acid. The slurry obtained was dried overnight at 50°C in an oven. GO powder was dissolved in double-distilled water and dispersed using a tip horn sonicator (Branson 550). The GO solution was obtained after centrifuging the dispersion (8000 rpm for 30 min) and collecting the supernatant (Table 1).

2.2 | GO/DSPC monolayer studies

2.2.1 | GO/DSPC Langmuir-Blodgett films fabrication

GO was diluted to $100 \mu\text{g ml}^{-1}$ n Milli-Q water. DSPC was acquired from Avanti Polar Lipids. Langmuir-Blodgett films with DSPC were obtained in a minitrough with area of $5 \times 19.5 \text{ cm}^2$ (KSV NIMA), housed in a 10,000 class cleanroom. The aqueous subphase was supplied by a Milli-Q purification system from Millipore (resistivity of $18.3 \text{ M}\Omega \text{ cm}$). All the measurements were performed at 22°C in subphase with pH 6.7.

To obtain the Langmuir-Blodgett films, $100 \mu\text{l}$ of the GO solution was diluted at the subphase. Next, $15 \mu\text{l}$ of typical 0.5 mg ml^{-1} concentration of DSPC in chloroform was spread on the subphase surface, followed by a 15 min incubation time to allow solvent evaporation. Fluorine tin oxide (FTO) substrate was removed from the subphase at a speed $\sim 1 \text{ mm min}^{-1}$ under surface pressure at

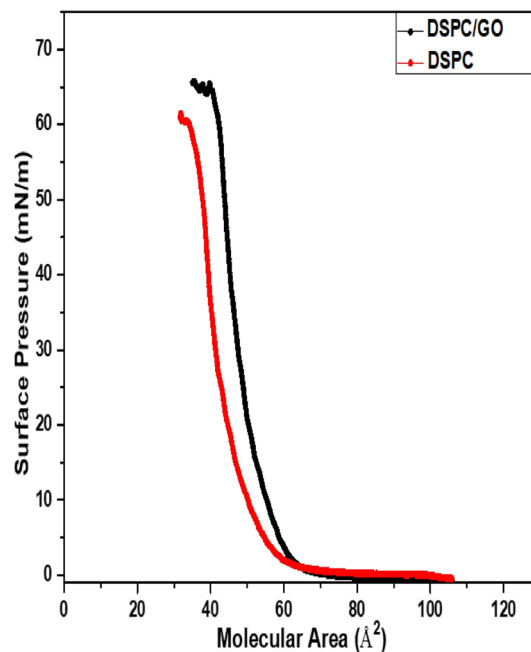


FIGURE 1 Surface pressure-area isotherms for DSPC and DSPC/GO systems. DSPC was spread on the subphase with or without GO and left for 15 min before compression. The barriers were compressed at a rate of 10 mm min^{-1} until the collapse of the membrane

$\sim 33 \text{ mN m}^{-1}$. Interactions between the monolayers and GO were investigated by Langmuir isotherms, as displayed in Figure 1, which shows the surface pressure isotherms containing DSPC and DSPC/GO, after the incubation with $0.2 \mu\text{g ml}^{-1}$.

2.2.2 | SFG spectroscopy

Sum frequency generation (SFG) spectra were obtained with a commercial SFG spectrometer (EKSPLA, Lithuania) by in situ measurements using the same experimental procedure described by Uehara et al.²⁷ Briefly, an active-passive mode-locked Nd+3:YAG laser generates 30 ps pulses at a wavelength of 1064 nm (repetition rate of 20 Hz). It pumps a harmonic generator unit that produces the second- (532 nm) and third-harmonic (355 nm). Part of the visible beam (532 nm) is used to excite the sample, together with a tunable Infrared (IR) pulse (from 4000 to 1000 cm^{-1} , bandwidth 3 cm^{-1}) generated by an optical parametric generator/optical parametric amplifier pumped

at 355 nm, coupled to a difference-frequency generation stage which is pumped by 1064 nm. SFG signal in the reflection geometry is generated by overlapping the visible and IR pulses in the same spot ($\sim 1 \text{ mm}^2$) and time at the interface. The incidence angles and pulse energies of the visible and infrared input beams are $60^\circ/\sim 700 \mu\text{J}$ and $55^\circ/50\text{--}150 \mu\text{J}$, respectively. SSP polarization combination was used (S-polarized SFG output, S-polarized visible input, P-polarized infrared input). Polarization S and P represents the component of the electric field, which are perpendicular and parallel to the incidence plane, respectively.²⁸

2.3 | Electrospun nanofibers

For fabricating the electrospun nanofibers, PLC (MW: 80,000, Sigma-Aldrich, MO, USA) was dissolved (4 wt% in respect to the solvent mixture) in a mixture of chloroform and methanol (both purchased from J. T. Baker) (3:1 v/v). The polymer solution was infused at a rate of

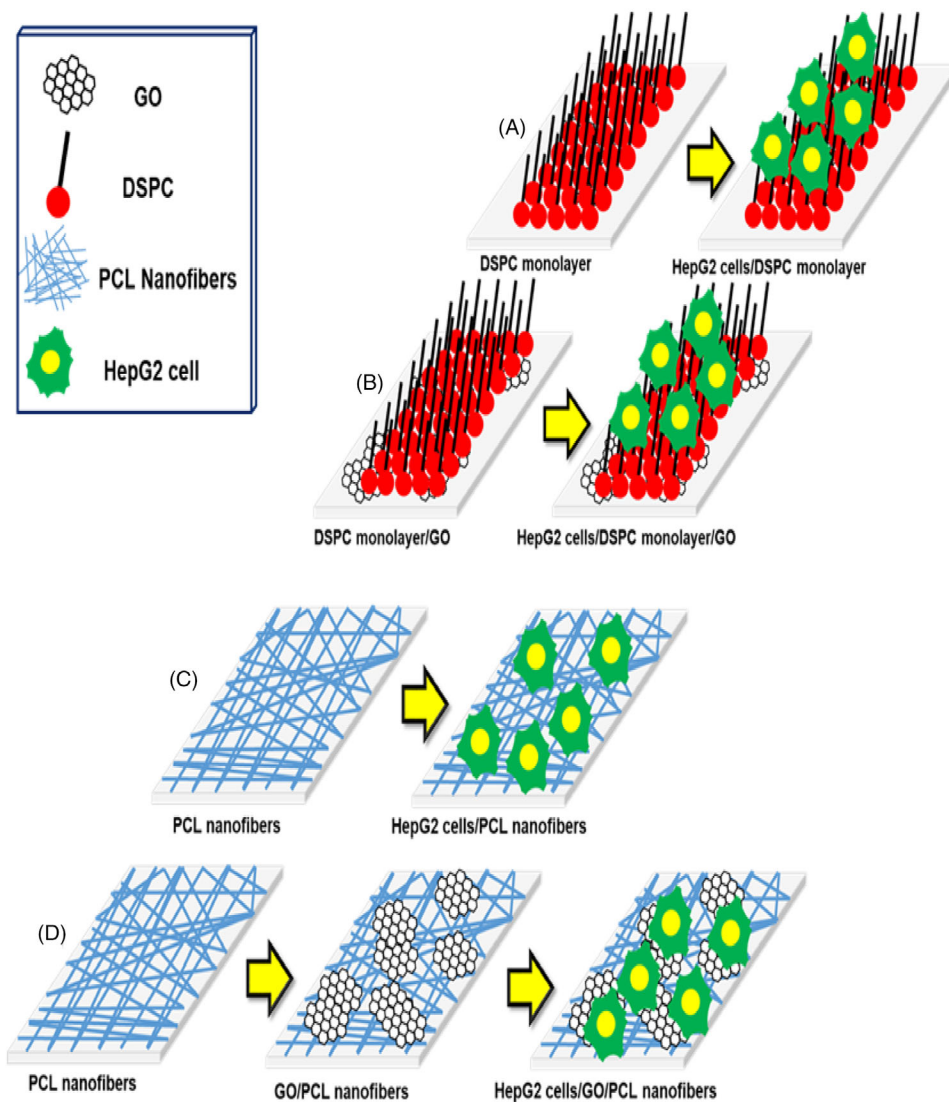


FIGURE 2 (A) HepG2 cells on DSPC monolayer (HepG2 cells/DSPC monolayer). (B) HepG2 cells on DSPC monolayer/GO (HepG2 cells/DSPC monolayer/GO). (C) HepG2 cells on PCL nanofibers (HepG2 cells/PCL nanofibers). (D) HepG2 cells on GO/PCL nanofibers (HepG2 cells/GO/PCL nanofibers)

0.3 ml h⁻¹ through a metallic needle (18G-1 gauge, inner diameter: 1.2 mm), and an electrical voltage of 20 kV was employed for electrospinning the nanofibers^{29–31} using a working distance of ~15 cm. The environment relative humidity during the electrospinning process was maintained at 60% (using silica gel). Electrospun nanofibers were ejected from the needle onto the fluorine doped tin oxide (FTO) substrate. The electrospinning time for random deposition was set as 25 min, with a deposition rate of 0.3 ml h⁻¹. In this situation, the electrospinning collection time was set as 25 min.

After the electrospinning process, the scaffolds formed by the nanofibers were modified with oxygen plasma (SPI Plasma Prep II—West Chester, PA, USA) for 90 s (Tension 50 V) to change their hydrophilic surface in order to enhance the interaction with GO.³²

For contact angle experiments, a goniometer (CAM 2008, KSV—equipped with CAM 2008 software) was employed. The samples (~15 mm × 10 mm) were attached to glass slides, and the contact angles were obtained from the profile droplets (~3 μl) using deionized water, ethylene glycol, and diiodomethane. Each sample was evaluated at three different points at room temperature. The contact angle data and the surface tension components of the probe liquids ($\gamma_L, \gamma_L^{LW}, \gamma_L^-, \gamma_L^+$) were evaluated using the Oss, Chaudhery, and Good model^{33,34} to obtain the free energy (ΔG), allowing the evaluation of hydrophobicity or hydrophilicity of surface.³⁵

The electrospun nanofibers were immersed for 1 h in the GO dispersion at concentrations of 100 μg ml⁻¹, and then dried at room temperature before initiate the cell investigations. Structurally, GO is planar with functionalization of carboxylic acid groups, allowing interaction with cells lineage and nanomaterials.³²

2.4 | Cancer liver cells culture on the nanoscaffolds

Cancer liver cells (HepG2 cells) were purchased from Cells Bank (Rio de Janeiro, Brazil). The cells were cultured using different densities: 5×10^2 , 5×10^3 , and 5×10^4 cells cm⁻², similar to what has been described by Zheng et al.²¹ In our studies, HepG2 cells were washed three times with phosphate buffered saline (PBS) and fixed with 5%

glutaraldehyde solution (50 wt% in H₂O, Sigma-Aldrich) for 30 min. The samples were then washed with distilled water during 5 min and carefully dehydrated by immersion in increasing concentrations (30%, 50%, 70%, 80%, 90%, 95%, and 100% of ethanol solution for 5 min). Figure 2 illustrates the sequence used with the respective nomenclature for producing the distinct scaffolds containing: (a) HepG2 cells on DSPC monolayer, (b) HepG2 cells on DSPC monolayer/GO, (c) HepG2 cells on PCL nanofibers, and (d) HepG2 cells on GO/PCL nanofibers.

Immunostaining³² was employed to evaluate the morphology of the cells. The procedure consisted in inserting the scaffolds in a formaldehyde solution (3.7%) for 30 min. After three washes in PBS, they were inserted in bovine serum albumin (BSA 2%) for 15 min and three additional PBS washes were performed. The samples were gold-coated (15 nm-thickness) using a sputterer (Leica EM SCD050) and imaged using scanning electron microscopy (SEM—FEG, ZEISS SIGMA model) to evaluate the morphologies of the cells on the electrospun fibers.

2.5 | Impedance spectroscopy measurements

Electrochemical experiments were employed to investigate the ability of the cancer cells to cover the nanostructured scaffolds surface. The

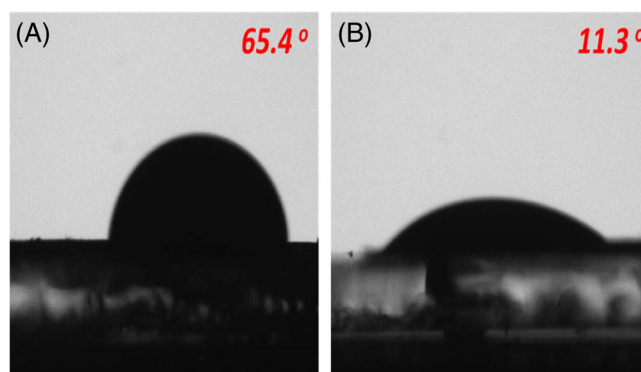


FIGURE 4 Contact angle measurement of PCL nanofibers scaffolds fabricated by electrospinning: (A) Before plasma treatment. (B) After oxygen plasma treatment [Corrections made on 23 November 2021, after first online publication: Figure labels have been added in the image to improve clarity.]

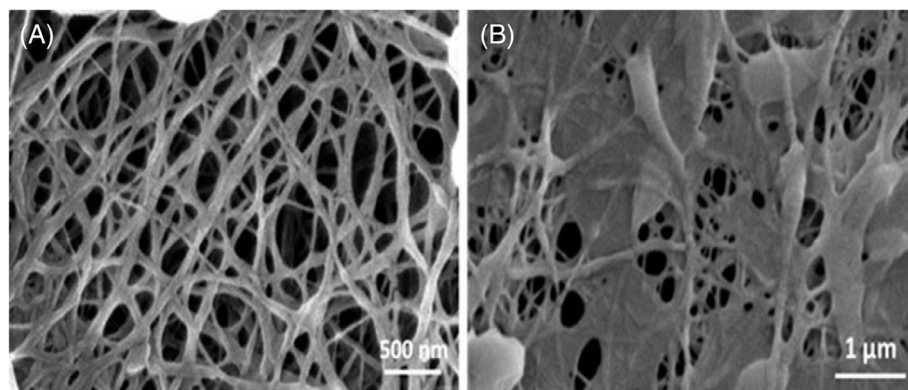
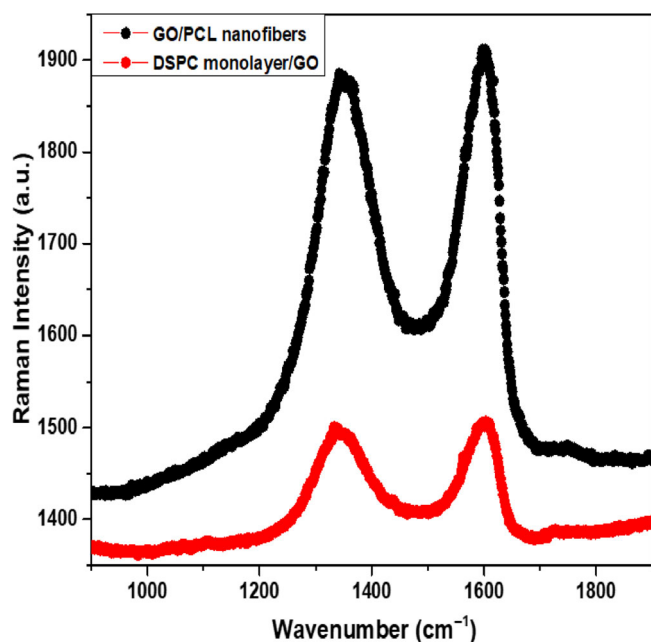


FIGURE 3 Scanning electron microscopy images: (A) PCL nanofibers and (B) GO/PCL nanofibers [Corrections made on 23 November 2021, after first online publication: Figure labels have been added in the image and the caption has been corrected to improve clarity.]

TABLE 2 Values of the surface tension components and parameters of the liquids used for contact angle

Liquids	γ^{LW}	γ^-	γ^+	γ^{AB}	γ^{TOTAL}	ΔG (mJ M ⁻²)
Water	21.8	25.5	25.5	51	72.8	-163.73
Ethylene glycol	29	47	1.92	19	48	-165.49
Diiodomethane	50.8	0	0	0	50.8	-165.45

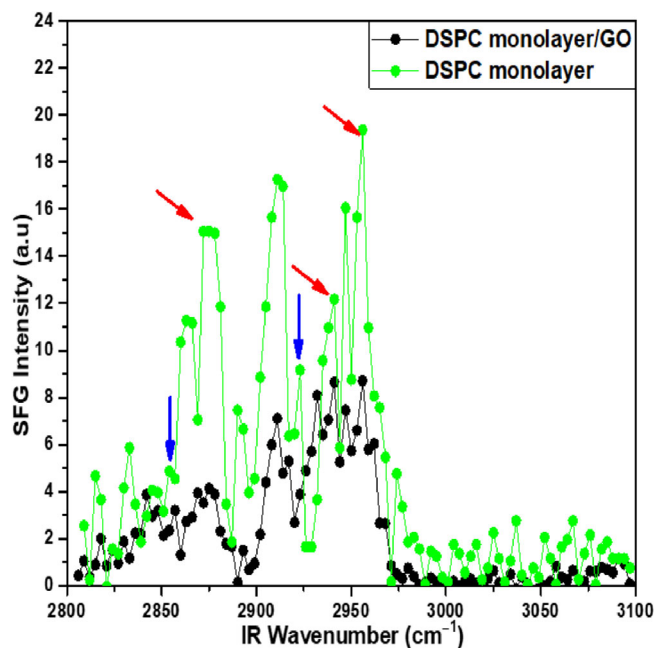
**FIGURE 5** Raman spectra of DSPC monolayer/GO and GO/PCL nanofibers scaffolds [Correction added on 23 November, after first online publication: An incorrect caption has been used in the original publication. This has been corrected.]

EIS experiments were carried out using a potentiostat PGSTAT Autolab (Metrohm) with Nova software (1.10). Ag/AgCl (3 mol L⁻¹ KCl) and platinum (Pt) foil were employed as the reference (RE) and counter (CE) electrodes, respectively, while modified fluorine doped tin oxide electrodes (FTO) (area of ~0.5 cm²) were employed as the working electrode. The modified FTO working electrodes used in the EIS experiments were: (i) Neat FTO (control), (ii) GO/FTO, (iii) DSPC monolayer/FTO, (iv) DSPC monolayer/GO/FTO, (v) PCL nanofibers/FTO, and (vi) GO/PCL nanofibers/FTO. HepG2 cells were immobilized on all the modified electrodes prior to the EIS experiments. The electrochemical impedance spectroscopy (EIS) measurements were obtained in 0.1 mol L⁻¹ KCl containing 0.05 mol L⁻¹ [Fe(CN)₆]^{3-/4-} at an open circuit potential over the frequency range from 0.1 Hz to 100 kHz, using a voltage amplitude of 10 mV.

3 | RESULTS AND DISCUSSION

3.1 | GO-modified electrospun nanofibers

Electrospun nanofiber mats produced by electrospinning are highly promising materials for fabricating scaffolds for tissue engineering

**FIGURE 6** SFG spectra of DSPC monolayer and DSPC monolayer/GO (incubation with GO containing 100 μg mL⁻¹) on FTO [Correction added on 23 November, after first online publication: An incorrect caption has been used in the original publication. This has been corrected.]

because of their correspondences to natural ECM fibrils.³⁶⁻³⁸ SEM images of random PCL nanofibers mats produced by electrospinning are displayed in Figure 3A, and the average diameters were estimated ~90 ± 47 nm (coherency ~9%), using the Image J software. Figure 3B shows a typical SEM image of random PCL nanofibers modified with GO 100 μg mL⁻¹, detailing the interaction between GO and PCL nanofibers after the plasma treatment.

Contact angle measurements were employed to confirm the change of hydrophobicity of the nanofibers surface after plasma treatment. Figure 4 shows that the contact angle for the PCL nanofibers decreased from 65.4 to 11.3° after the plasma treatment, confirming that the polymeric surface became more hydrophilic.

Through the method proposed by Good, van Oss, and Chaudhry,³³ contact angle measurements enabled to determine the nonwovens surface free energy parameters (Table 2) by probing three liquids (water, ethylene glycol, and diiodomethane).³⁹ Different interfacial process (absorption and wetting of aqueous fluids) are determined by the surface free energy components of nonwovens, and consequently can influence the final applications. γ^{LW} and γ^{AB} are related to apolar and polar interactions, respectively, contributing to the total surface energy γ^{TOTAL} . A similar parameter was analyzed on

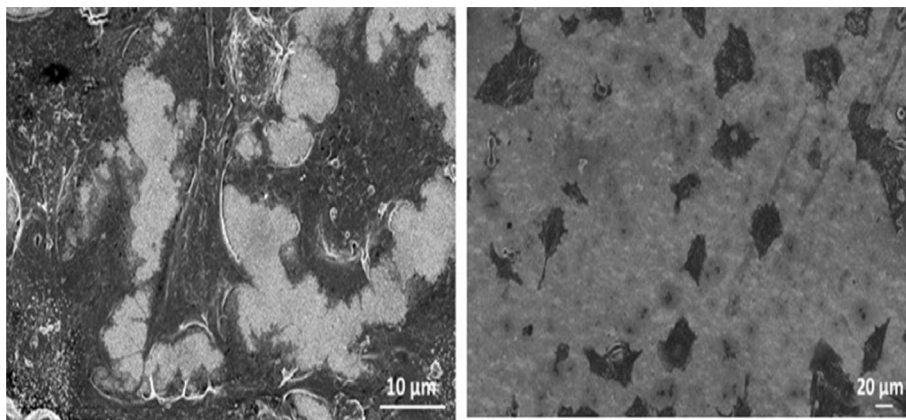


FIGURE 7 Scanning electron microscopy images of HepG2 cells [Correction added on 23 November, after first online publication: An incorrect caption has been used in the original publication. This has been corrected.]

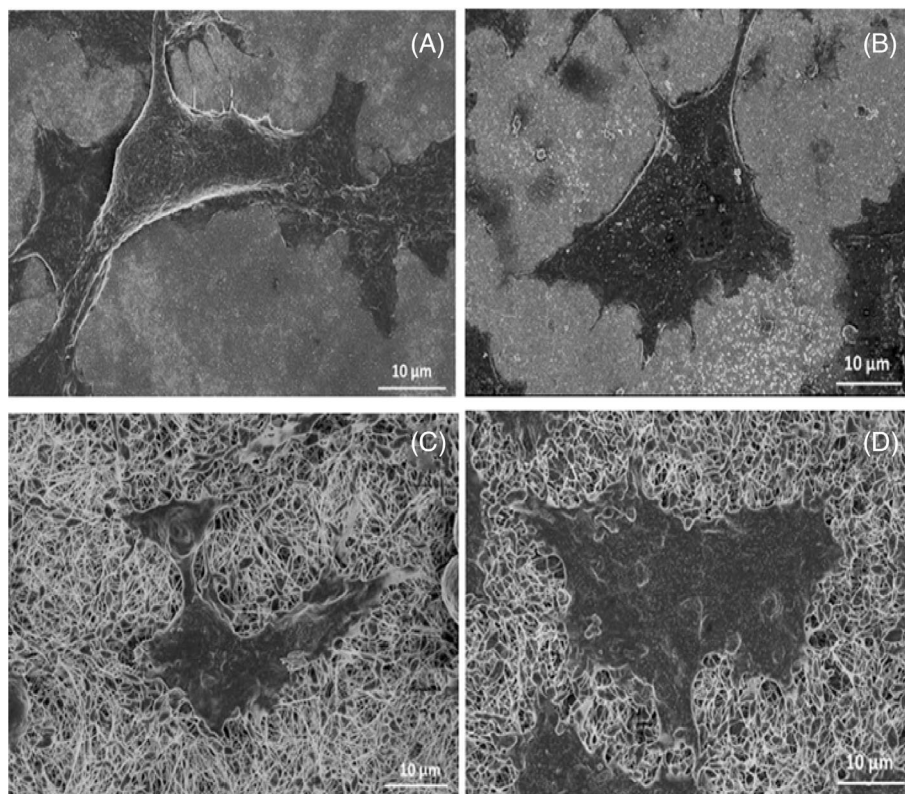


FIGURE 8 Scanning electron microscopy images of HepG2 cells on: (A) DSPC monolayer/GO; (B) GO; (C) PCL nanofibers; (D) GO/PCL nanofibers [Correction added on 23 November, after first online publication: The incorrect caption and duplicate figure label A have been corrected in this version.]

the electron-donor component (γ^-) of the polar surface energy on the electron-acceptor (γ^+) one ($\gamma^-/\gamma^+ \gg 1$), indicating that the surface of nonwovens has strong electron donating capacity to contribute in polar with acid solutions.^{34,35}

The interfacial free energy (ΔG) of the nonwovens was calculated in order to understand the nature of their surface (hydrophilic or hydrophobic). According to the thermodynamic convention, when the interaction of the material surface with water dominates, $\Delta G > 0$, and the surface of the material is hydrophilic. On the other hand, when the interaction of surface components of the material is benefited rather than developing an interface with water, $\Delta G < 0$, yielding hydrophobic surfaces.

Raman spectroscopy analyses confirmed the presence of GO/PCL nanofibers and DSPC monolayer/GO scaffolds, by investigating the functional GO groups as displayed in Figure 5. The bands at 1350 and

1600 cm^{-1} were observed, which are characteristics of the D and G bands from GO, respectively.^{32,40} These resonances are more intense for PCL nanofibers scaffolds containing a larger amount of GO due to the change of physical-chemical surface after plasma treatment. The high surface area to volume ratio of the nanofibers in conjunction with the 3D architecture results in high GO loading capacity.^{32,40}

3.2 | SFG spectroscopy

SFG spectroscopy was applied to characterize the formation of the DSPC monolayer and DSPC monolayer/GO on the FTO substrate. Furthermore, this technique is also important to understand the packing and molecular interactions between lipids and nanomaterials. The spectra for the DSPC monolayer and DSPC monolayer/GO in Figure 6

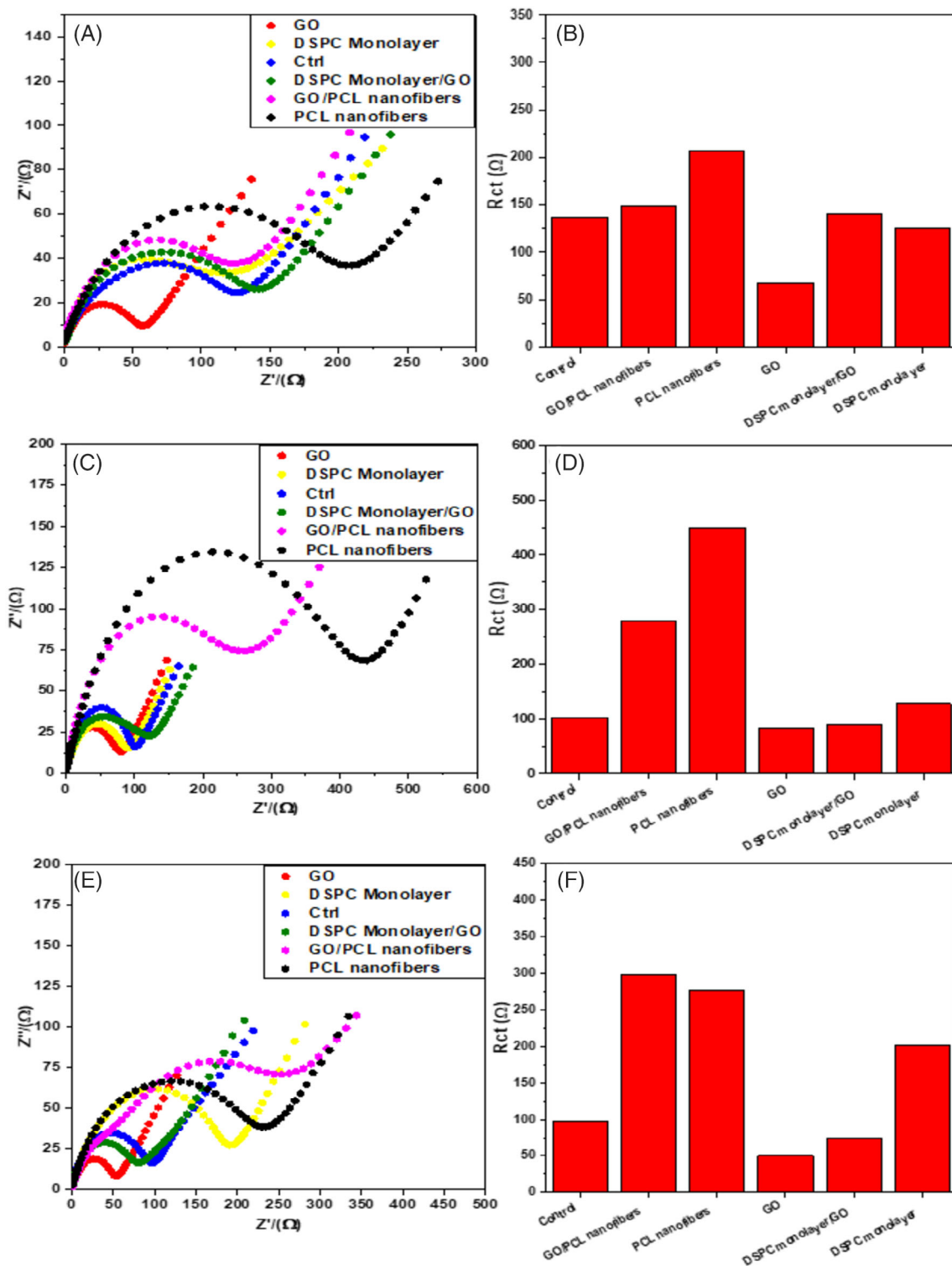


FIGURE 9 Nyquist plot (a), (c) and (e) and charge transfer resistance (R_{ct}) (b), (d) and (f) of GO, DSPC monolayer, control, DSPC monolayer/GO, GO/PCL nanofibers and PCL nanofibers scaffolds modified with different HepG2 cells densities: (a-b) 5×10^3 cells cm^{-2} ; (c-d) 5×10^4 cells cm^{-2} and (e-f) 5×10^5 cells cm^{-2} [Correction added on 23 November, after first online publication: An incorrect caption has been used in the original publication. This has been corrected.]

shows high-intensity resonances at 2879, 2945, and 2960 cm^{-1} (red arrows). These resonances are due to the symmetric stretch and its Fermi resonance with the overtone of the symmetric bending mode, and the asymmetric stretch of the CH_3 terminal group from alkyl chains

of phospholipids.⁴¹⁻⁴³ The spectra for DSPC/GO at 2850 and 2920 cm^{-1} (blue arrows), it is shown the CH_2 symmetric and asymmetric stretches from lipid chains, respectively.⁴³ It is possible to infer the formation of an expanded phospholipid monolayer, with some

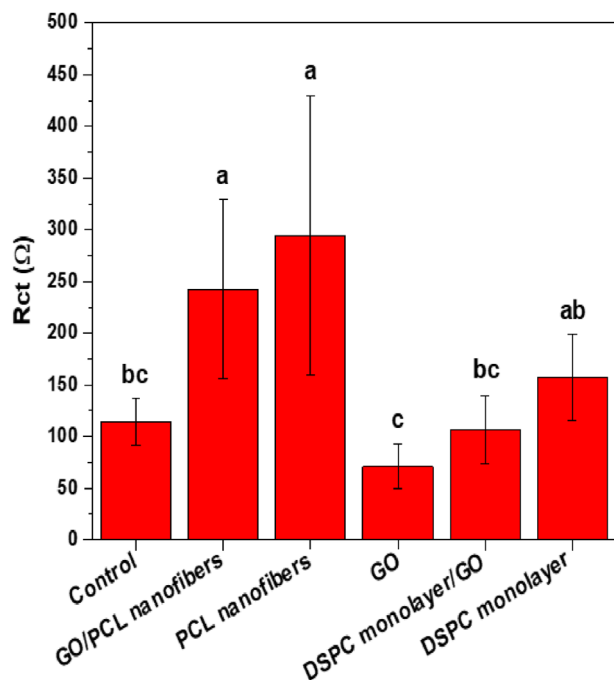


FIGURE 10 Charge transfer resistance (R_{ct}) of HepG2 cells density average (5×10^3 , 5×10^4 , and 5×10^5 cells cm^{-2}) on: GO/PCL nanofibers, PCL nanofibers, GO, DSPC monolayer/GO, and DSPC monolayer. Kruskal–Wallis test at the 95% confidence level differ means followed by the same letter in the columns

organization and orientation of the lipid tails but with several *gauche* defects. The reason for this more expanded structure for the lipid monolayer may be the interaction of the polar headgroups with the GO, which is then transferred to the FTO substrate underneath the DSPC film.⁴⁴

3.3 | HepG2 cells adhesion on the nanostructured scaffolds

Following incubation of HepG2 cells/PCL nanofibers and HepG2 cells/DSPC monolayer, both with GO ($100 \mu\text{g ml}^{-1}$) for 6 days, the cells were analyzed using SEM images. Figure 7 illustrates the control (HepG2 cells only) on neat scaffold. For both systems, HepG2 cells did show a regular morphology, without the interference of nanomaterials.

Figure 8A–D illustrate the morphology of HepG2 cells on DSPC monolayer/GO, GO, GO/PCL nanofibers, and GO/PCL nanofibers, respectively. In all the scaffolds systems, the cells adhered and grew on different surfaces with a similar morphology.

The adhesion and growth of the cells on the nanofiber scaffolds was analyzed using EIS. Nyquist plots for neat FTO substrate (control), GO, DSPC monolayer/GO, DSPC monolayer, PCL nanofibers, and GO/PCL nanofibers are illustrated in Figure 9 for different density of cells. The density of HepG2 cells used were 5×10^3 , 5×10^4 , and 5×10^5 cells cm^{-2} , and are represented in Figure 9A–C, respectively.

Randle's equivalent circuit model was used to fit the experimental data, where R_s , R_{ct} , C_{dl} , and Z_w represent the electrolyte resistance, the charge transfer resistance, the interface capacitance, and the Warburg impedance, respectively. The interfacial transfer process concerns to the semicircular region located at high frequencies, from which the charge transfer resistance (R_{ct}) can be inferred from the diameter of the semicircle, while the linear region, at low frequencies, is related to the diffusional process.

Scaffolds systems with PCL nanofibers and GO/PCL nanofibers presented higher charge transfer resistance, while DSPC monolayer and DSPC monolayer/GO scaffolds exhibited an electron transfer similar to the control sample (neat FTO), except for DSPC monolayer scaffold and control sample containing high density of cells ($\sim 10^5$ cells cm^{-2}).

Scaffolds containing neat GO exhibited the best electron transfer rate due to the conductivity of this nanomaterial.

Figure 10 shows the charge transfer resistance (R_{ct}) of HepG2 cells density average (5×10^3 , 5×10^4 , and 5×10^5 cells cm^{-2}) on: Neat FTO (control), GO/FTO, DSPC monolayer/FTO, DSPC monolayer/GO/FTO, PCL nanofibers/FTO, and GO/PCL nanofibers/FTO samples. The values are expressed as mean value \pm standard deviation, where statistical analysis was carried out using analysis of Kruskal–Wallis test, (95% confidence level using R Software). The comparative statistical analyses revealed that GO/PCL nanofibers and PCL nanofibers presented superior R_{ct} values compared to other samples (control, GO, DSPC monolayer/GO, and DSPC monolayer). Indicating deficiencies to promote electron transfer. Furthermore, by increasing the HepG2 cells density (10^4 and 10^5 cell cm^{-2}) on GO/PCL nanofibers, the quantity of cells influenced the charge transfer resistance, increasing the respective values.

4 | CONCLUSIONS

DSPC monolayers and biodegradable PCL nanofibers were produced by Langmuir–Blodgett and electrospinning techniques, respectively, which were further modified with GO to be used as cancer liver cells scaffolds. Raman spectroscopy revealed the presence of GO on the nanofibers surface and under phospholipids monolayer, while SFG indicated the presence of the DSPC monolayers, detailing their ordering with GO. According to Nyquist plots, PCL nanofibers scaffolds showed the highest charge transfer resistance. DSPC monolayer and DSPC monolayer/GO did not interfere on charge transfer resistance, resulting in values similar to the control sample. Our results indicate that the as-developed scaffolds containing different nanoarchitectures impact on the electron transfer on liver cancer cells. Therefore, the interactions between the surface containing nanostructures depend on the physical/chemistry properties of polymer nanofibers or Langmuir monolayer, which aspect should be carefully evaluated when these nanostructures are intended for regenerative medicine applications.

ACKNOWLEDGMENTS

The authors thank the financial support from Brazilian National Council for Scientific and Technological Development (CNPq: 155449/2018-4 and 155449/2016-2), São Paulo Research Foundation (FAPESP: 2017/10582-8, 2018/02819-0, 2017/21791-7, 2017/12174-4, 18/22214-6), MCTI-SisNano (CNPq/402.287/2013-4), Coordination for the Improvement of Higher Education Personnel (CAPES) - Funding Code 001 and AgroNano research (EMBRAPA) from Brazil.

CONFLICT OF INTEREST

The authors declare no conflict of interest.

DATA AVAILABILITY STATEMENT

The data that support the findings of this study are available from the corresponding author upon reasonable request.

ORCID

Thiers M. Uehara  <https://orcid.org/0000-0001-5790-0673>

Fernanda L. Migliorini  <https://orcid.org/0000-0002-9605-2790>

Murilo H. M. Facure  <https://orcid.org/0000-0003-0858-0364>

Nicolau B. Palma Filho  <https://orcid.org/0000-0003-4625-4332>

Paulo B. Miranda  <https://orcid.org/0000-0002-2890-0268>

Valtencir Zucolotto  <https://orcid.org/0000-0003-4307-3077>

Daniel S. Correa  <https://orcid.org/0000-0002-5592-0627>

REFERENCES

- Besinis A, De Peralta T, Tredwin CJ, Handy RD. Review of nanomaterials in dentistry: interactions with the oral micro-environment, clinical applications, hazards, and benefits. *ACS Nano*. 2015;9:2255-2289.
- Xu J, Gulzar A, Yang D, Gai S, He F, Yang P. Tumor self-responsive upconversion nanomedicines for theranostic applications. *Nanoscale*. 2019;11:17535-17556.
- Mosquera J, García I, Liz-Marzán LML. Cellular uptake of nanoparticles versus small molecules: a matter of size. *Acc Chem Res*. 2018;51:2305-2313.
- Zhang Y, Fang L, Cao Z. Atomically dispersed Cu and Fe on N-doped carbon materials for CO₂ electroreduction: insight into the curvature effect on activity and selectivity. *RSC Adv*. 2020;10:43075-43084.
- Lett JA, Sagadevan S, Fatimah I, et al. Recent advances in natural polymer - based hydroxyapatite scaffolds: properties and applications. *Eur Polym J*. 2021;148:110360.
- Liu L, Zhang J, Zhao J, Liu F. Mechanical properties of graphene oxides. *Nanoscale*. 2012;4:5910-5916.
- Mei Q, Liu B, Han G, Liu R, Han MY, Zhang Z. Graphene oxide: from tunable structures to diverse luminescence behaviors. *Adv Sci*. 2019;6:1900855.
- Chen J, Li L. Effect of oxidation degree on the thermal properties of graphene oxide. *J Mater Res Technol*. 2020;9:13740-13748.
- Zheng N, Song Y, Wang L, Gao J, Wang Y, Dong X. Improved electrical and mechanical properties for the reduced graphene oxide-decorated polymer nanofiber composite with a Core-Shell structure. *Ind Eng Chem Res*. 2019;58:15470-15478.
- Kim SG, You NH, Ku BC, Lee HS. Polyvinylidene fluoride/reduced graphene oxide on SiO_xN_y/poly(ethylene terephthalate) films as transparent coatings for organic electronic devices and packaging materials. *ACS Appl Nano Mater*. 2020;3:8972-8981.
- Kühnel M, Petersen SV, Hviid R, Overgaard MH, Laursen BW, Nørgaard K. Monolayered graphene oxide as a low contact resistance protection layer in Alkanethiol solid-state devices. *J Phys Chem C*. 2018;122:9731-9737.
- Shi HTH, Jang S, Naguib HE. Freestanding laser-assisted reduced graphene oxide microribbon textile electrode fabricated on a liquid surface for supercapacitors and breath sensors. *ACS Appl Mater Interfaces*. 2019;11:27183-27191.
- Roy K, Ghosh SK, Sultana A, et al. Self-powered wearable pressure sensor and pyroelectric breathing sensor based on GO interfaced PVDF nanofibers. *ACS Appl Nano Mater*. 2019;2:2013-2025.
- Jiang S, Chen Y, Duan G, Mei C, Greiner A, Agarwal S. Electrospun nanofiber reinforced composites: a review. *Polym Chem*. 2018;9:2685-2720.
- Zhou X, Ding C, Cheng C, et al. Mechanical and thermal properties of electrospun polyimide/rGO composite nanofibers via in-situ polymerization and in-situ thermal conversion. *Eur Polym J*. 2020;141:110083.
- Cleeton C, Keirouz A, Chen X, Radacsi N. Electrospun nanofibers for drug delivery and biosensing. *ACS Biomater Sci Eng*. 2019;5:4183-4205.
- Creighton RL, Phan J, Woodrow KA. In situ 3D-patterning of electrospun fibers using two-layer composite materials. *Sci Rep*. 2020;10:7949.
- Jin L, Xu Q, Wu S, et al. Synergistic effects of conductive three-dimensional Nanofibrous microenvironments and electrical stimulation on the viability and proliferation of Mesenchymal stem cells. *ACS Biomater Sci Eng*. 2016;2:2042-2049.
- Yablonka-Reuveni Z, Nameroff M. Skeletal muscle cell populations. *Histochemistry*. 1987;87:27-38.
- Biazar E. Application of polymeric nanofibers in soft tissues regeneration. *Polym Adv Technol*. 2016;27:1404-1412.
- Zheng TT, Zhang R, Zou L, Zhu JJ. A label-free cytosensor for the enhanced electrochemical detection of cancer cells using polydopamine-coated carbon nanotubes. *Analyst*. 2012;137:1316-1318.
- Cancino J, Paino IMM, Micocci KC, Selistre-de-Araujo HC, Zucolotto V. In vitro nanotoxicity of single-walled carbon nanotube-dendrimer nanocomplexes against murine myoblast cells. *Toxicol Lett*. 2013;219:18-25.
- Holle AW, Young JL, Spatz JP. In vitro cancer cell-ECM interactions inform in vivo cancer treatment. *Adv Drug Deliv Rev*. 2016;97:270-279.
- Mercante LA, Facure MHM, Locilento DA, et al. Solution blow spun PMMA nanofibers wrapped with reduced graphene oxide as a highly efficient dye adsorbent. *New J Chem*. 2017;41:9087-9094.
- Huo D, Li Q, Zhang Y, Hou C, Lei Y. A highly efficient organophosphorus pesticides sensor based on CuO nanowires-SWCNTs hybrid nanocomposite. *Sens Actuators B*. 2014;199:410-417.
- Chen J, Yao B, Li C, Shi G. An improved hummers method for eco-friendly synthesis of graphene oxide. *Carbon*. 2013;64:225-229.
- Uehara TM, Marangoni VS, Pasquale N, Miranda PB, Lee KB, Zucolotto V. A detailed investigation on the interactions between magnetic nanoparticles and cell membrane models. *ACS Appl Mater Interfaces*. 2013;5:13063-13068.
- Shen YR. Optical second harmonic generation at interfaces. *Annu Rev Phys Chem*. 1989;40:327-350.
- De Vrieze S, Westbroek P, Camp TV, Langenhove LV. Electrospinning of chitosan nanofibrous structures: feasibility study. *J Mater Sci*. 2007;42:8029-8034.
- Chen M, Wang C, Fang W, et al. Electrospinning of Calixarene-functionalized Polyacrylonitrile nanofiber membranes and application as an adsorbent and catalyst support. *Langmuir*. 2013;29:11858-11867.
- Tripatanasuwana S, Zhong Z, Reneker DH. Effect of evaporation and solidification of the charged jet in electrospinning of poly(ethylene oxide). *Polymer*. 2007;48:5742-5746.

32. Shah S, Yin PT, Uehara TM, Chueng STD, Yang L, Lee KB. Guiding stem cell differentiation into oligodendrocytes using graphene-nanofiber hybrid scaffolds. *Adv Mater.* 2014;26:3673-3680.
33. van Oss CJ, Chaudhury MK, Good RJ. Interfacial Lifshitz-van der Waals and polar interactions in macroscopic systems. *Chem Ver.* 1988;88:927-941.
34. van Oss CJ. Hydrophobicity of biosurfaces - origin, quantitative determination and interaction energies. *Colloids Surf B Biointerfaces.* 1995;5:91-110.
35. Rojo E, Peresin MS, Sampson WW, et al. Comprehensive elucidation of the effect of residual lignina on the physical, barrier, mechanical and surface properties of nanocellulose films. *Green Chem.* 2015;17:1853-1866.
36. Patel S, Kurpinski K, Quigley R, et al. Bioactive nanofibers: synergistic effects of Nanotopography and chemical signaling on cell guidance. *Nano Lett.* 2007;7:2122-2128.
37. Rouède D, Schaub E, Bellanger JJ, et al. Determination of extracellular matrix collagen fibril architectures and pathological remodeling by polarization dependente second harmonic microscopy. *Sci Rep.* 2017;7:1-12.
38. Sun L, Gao W, Fu X, et al. Enhanced wound healing in diabetic rats by nanofibrous mimicking the basketweave pattern of collagen fibrils in native skin. *Biomater Sci.* 2018;6:340-349.
39. Wu W, Giese RF Jr, van Oss CJ. Evaluation of the Lifshitz-van der Waals/Acid-Base approach to determine surface tension components. *Langmuir.* 1995;11:379-382.
40. Uehara TM, Paino IMM, Santos FA, Scagion VP, Correa DS, Zucolotto V. Fabrication of random and aligned electrospun nanofibers containing graphene oxide for skeletal muscle cells scaffold. *Polym Adv Technol.* 2020;31:1-7.
41. Snyder RG, Hsu SL, Krimm S. Vibrational spectra in the CH stretching region and the structures of the polymethylene chain. *Spectrochim Acta.* 1978;34A:395-406.
42. Lu R, Gan W, Wu B, Zhang Z, Guo Y, Wang H. C-H stretching vibrations of methyl, methylene and Methine groups at the vapor/alcohol (n= 1-8) interfaces. *J Phys Chem B.* 2005;109:14118-14129.
43. Guyot-Sionnest P, Hunt JH, Shen YR. Sum-frequency vibrational spectroscopy of a Langmuir film: study of molecular orientation of two-dimesnional system. *Phys Rev Lett.* 1987;59:1597-1600.
44. Liljeblad JFD, Bulone V, Rutland MW, Johnson CM. Supported phospholipid monolayers. The molecular structure investigated by vibrational sum frequency spectroscopy. *J Phys Chem C.* 2010;115:10617-10629.

How to cite this article: Uehara TM, Migliorini FL, Facure MHM, et al. Nanostructured scaffolds containing graphene oxide for nanomedicine applications. *Polym Adv Technol.* 2022;33(2):591-600. doi:10.1002/pat.5541